



Published in final edited form as:

*Int J Mass Spectrom.* 2017 November ; 422: 177–187. doi:10.1016/j.ijms.2017.03.010.

## Mars Organic Molecule Analyzer (MOMA) laser desorption/ionization source design and performance characterization

Xiang Li<sup>a,\*</sup>, Ryan M. Danell<sup>b</sup>, Veronica T. Pinnick<sup>a</sup>, Andrej Grubisic<sup>c</sup>, Friso van Amerom<sup>d</sup>, Ricardo D. Arevalo Jr.<sup>e</sup>, Stephanie A. Getty<sup>e</sup>, William B. Brinckerhoff<sup>e,\*</sup>, Adrian E. Southard<sup>f</sup>, Zachary D. Gonnens<sup>e</sup>, Tomoko Adachi<sup>g</sup>

<sup>a</sup>Center for Space Science & Technology, University of Maryland, Baltimore County, Baltimore, MD, USA

<sup>b</sup>Danell Consulting, Inc., Winterville, NC, USA

<sup>c</sup>Center for Research and Exploration in Space Science & Technology, University of Maryland, College Park, College Park, MD, USA

<sup>d</sup>Mini-Mass Consulting Inc., Hyattsville, MD, USA

<sup>e</sup>NASA Goddard Space Flight Center, Greenbelt, MD, USA

<sup>f</sup>Universities Space Research Association, Columbia, MD, USA

<sup>g</sup>Catholic University, Washington DC, USA

### Abstract

The Mars Organic Molecule Analyzer (MOMA), a dual-source, ion trap-based instrument capable of both pyrolysis-gas chromatography mass spectrometry (pyr/GC-MS) and laser desorption/ionization mass spectrometry (LDI-MS), is the core astrobiology investigation on the ExoMars rover. The MOMA instrument will be the first spaceflight mass analyzer to exploit the LDI technique to detect refractory organic compounds and characterize host mineralogy; this mode of analysis will be conducted at Mars ambient conditions. In order to achieve high performance in the Martian environment while keeping the instrument compact and low power, a number of innovative designs and components have been implemented for MOMA. These include a miniaturized linear ion trap (LIT), a fast actuating aperture valve with ion inlet tube, and a Microelectromechanical System (MEMS) Pirani sensor. Advanced analytical capabilities like Stored Waveform Inverse Fourier Transform (SWIFT) for selected ion ejection and tandem mass spectrometry (MS/MS) are realized in LDI-MS mode, and enable the isolation and enhancement of specific mass ranges and structural analysis, respectively. We report here the technical details of these instrument components as well as system-level analytical capabilities, and we review the applications of this technology to Mars and other high-priority targets of planetary exploration.

\*Corresponding authors. xiang.li@nasa.gov, shawnli@umbc.edu (X.Li), william.b.brinckerhoff@nasa.gov (W.B. Brinckerhoff).

## Keywords

Mars Organic Molecule Analyzer (MOMA); Laser desorption/ionization mass; spectrometry (LDI-MS); Miniaturized linear ion trap (LIT)

---

## 1. Introduction

The primary science goal of the joint ESA-Roscosmos ExoMars Program is to search for signs of past or present life on Mars through a detailed chemical analysis of the Martian atmosphere (via an orbiter launched in 2016) and surface (via a rover to be launched in 2020) [1]. The Mars Organic Molecule Analyzer (MOMA) is a key instrument on the Pasteur Payload of the ExoMars rover. MOMA is a lightweight (~12 kg), low power (75 W average), dual-ion source mass spectrometer-based instrument utilizing a miniaturized linear ion trap (LIT). MOMA supports two modes of operation: i) pyrolysis/gas chromatography mass spectrometry (pyr/GC-MS), and ii) laser desorption/ionization mass spectrometry (LDI-MS) at ambient Mars pressures [2]. Although the instrument has the capacity to measure inorganic compounds, such as rock-forming mineral oxides, the MOMA investigation is primarily focused on the detection and structural characterization of organic compounds that may be present in martian near-subsurface samples over a range of preservational environments, volatility, and molecular weight. Because the rover's drill can access samples from the surface down to 2m, MOMA will be able will examine the chemical composition of samples acquired at depths where organics may be protected from radiation, oxidation and other mechanisms of degradation [3]. In addition to enabling mission science, MOMA informs critical sampling strategies for future *in situ* analysis and Mars Sample Return (MSR).

The core of the mass analyzer, the LIT combines influences from commercial instrument design (e.g., Thermo Fisher LTQ) and from heritage quadrupole mass spectrometers (QMS) successfully qualified for spaceflight, flown and operated in a range of planetary environments (e.g., Sample Analysis at Mars (SAM) on Mars Science Laboratory). The LIT design minimizes mass, volume and power to meet stringent spaceflight constraints, while supporting novel customization including IDI of samples at Mars ambient conditions and utilization of the martian atmosphere for ion trapping and cooling. Furthermore, the LIT offers the ability to amplify signals from low abundance species as well as to perform structural characterization of complex molecules using multi-frequency waveforms and tandem mass spectrometry. Compared to classical 3D traps, the LIT geometry provides the following analytical advantages: symmetrical ion injection from either end of the rod assembly, thus simplifying the interfaces to both GC and LDI sources with a single analyzer; redundant detector channels to increase sensitivity and extend operational lifetime (reducing technical risk); and greater ion capacity.

Although MOMA will not be the first ion trap in space (VCAM on the International Space Station, ISS [4]), nor the first ion trap to explore another planetary body (Ptolemy onboard Rosetta's Philae lander [5]), the instrument will be the first to conduct LDI-MS on another solar system body. First developed in the early 1970's [6], the laser desorption/ionization

(LDI) technique became a common ionization method for mass spectrometric analysis beginning in the late 1980's [7,8] after the advent of matrix-assisted laser desorption/ionization (MALDI). The matrix is a chemical medium that strongly absorbs laser radiation (most commonly at ultraviolet, or UV wavelengths) causing it to be volatilized and to carry analyte molecules, typically with lower direct UV laser absorbance, into the gas phase, which are ionized mainly through proton transfer. However, many organic species, especially aromatic moieties, exhibit strong UV absorption: a pulsed laser can directly volatilize and photoionize such organic compounds in geological samples without any additional matrix [9,10]. For example, several carboxylic acids, aromatic amino acids, nucleobases, polycyclic aromatic hydrocarbons (PAHs), and kerogen-like or macromolecular carbon are all detectable through matrix-free LDI-MS. Therefore, the LDI technique is capable of providing valuable information about the chemical composition and structure of mid- to high molecular weight, generally nonvolatile, species, from hundreds up to thousands of Da. Lacking a requirement for multi-step chemical preparation of samples, this protocol is well suited for a broad-based investigation of potential molecular biosignatures on the resource-constrained ExoMars rover mission. In addition, the presence of selected low mass elemental, mineral oxide, sulfate and sulfide species can also be inferred, providing contextual information about the environment in which organics are preserved.

Outside of the LIT, a number of other innovative components have been developed for the MOMA instrument. These include a fast acting aperture valve with ion inlet tube, and a Microelectromechanical System (MEMS) Pirani pressure sensor to help conquer the challenges of realizing LDI-MS mode at Mars ambient pressure. End-to-end LDI-MS operation including these components has been validated [2,11] by functional testing on multiple breadboard prototypes, the engineering test unit (ETU), and the flight model (FM). Multiple levels of integration and test are still underway prior to delivery and installation of MOMA into the ExoMars rover. Here in this report, we will present technical details of the LDI-MS mode of operation and related components on MOMA.

## 2. Challenges for using an LIT in the martian environment

For decades, quadrupole mass spectrometer (QMS) instruments designed, built and tested at NASA's Goddard Space Flight Center have been deployed on missions to explore the inner and outer solar system, including: Venus (e.g., Pioneer Venus [12]); the Moon (e.g., LADEE [13]); Mars (e.g., MSL [14] and MAVEN [15]); Jupiter and its satellites (Galileo [16,17]); and the Saturnian system (e.g., Cassini-Huygens [18]). All of these instruments relied on high vacuum conditions (base pressures  $<10^{-6}$  Pa) to address fundamental mission requirements and maximize science return. In contrast, ion traps operate nominally at moderate pressures (on the order of  $10^{-1}$  Pa) as collisions between analyte and background gas serve to attenuate the kinetic energy of (or, "cool") the ions of interest. To simplify design and minimize consumables, MOMA makes use of the predominantly  $\text{CO}_2$  martian atmosphere, at  $\sim 1$  kPa ( $\sim 7$  Torr), as a cooling gas, as opposed to the usual He, presenting some specific challenges to the instrument operation. In addition to the challenges associated with operating high voltages at relatively high pressures, the presence of a heavier  $\text{CO}_2$ -dominated background gas composition (specifically containing 96%  $\text{CO}_2$ , 2% Ar and 2%  $\text{N}_2$  [19]) during LDI-MS operations can interfere with ion ejection and cause a decrease in

mass spectral resolution [20]. A significant shift away from traditional design practices was therefore required to optimize the MOMA instrument. Furthermore, the elevated operating pressure in a the small LIT housing required that meticulous attention be paid to component geometries (e.g., via field modeling), minimizing sharp edges and controlling surface finishes of manufactured parts, material properties (e.g., outgassing), and potential virtual leaks in order to maintain low field gradients and thus promote high-voltage stability.

### 3. LDI mode operation

The LDI technique was one of the first ionization sources coupled to a mass spectrometer that enabled detection of large intact molecules (kDa or more) due to the “soft” nature of the laser irradiation, which results in low analyte fragmentation [21,22]. The focus of the LDI-MS mode for the MOMA investigation is the detection and structural analysis of primarily nonvolatile organic compounds up to 1 kDa. The drill system on the ExoMars rover extracts materials from as deep as 2m. Vertical surveys will be conducted in which samples are collected from 0, 50, 100, 150, and 200 cm depths in one location. Crushed rock aliquots derived from each drill collection are sent through the rover’s Sample Processing and Distribution System (SPDS), which doses fines either into an oven (for GCMS) or onto a refillable tray. The tray is mounted on a carousel which then positions the sample under the MOMA ion inlet system, all under Mars ambient conditions (0.5–1 kPa, or 4–8 Torr Mars atmosphere [23]) for in situ laser analysis. The solid-state, frequency-quadrupled Nd:YAG MOMA laser generates 266nm wavelength radiation in ns pulses at energies up to 130μJ per pulse; the output energy may be attenuated in 10% increments down to 13 uJ/pulse via thermal detuning of the fourth harmonic nonlinear optical crystal. The laser beam is introduced at an incident angle of ~45° relative to the sample surface, and focused to an elliptical spot size with a major axis diameter of 600 μm. This beam profile produces fluences on the order of 0.01 – 0.1 J•cm<sup>-2</sup>, and irradiances of 10 – 100 MW•cm<sup>-2</sup>. The laser can generate up to 50 pulses at a repetition rate of 100 Hz, but due to thermal limitations on the duty cycle, the laser must maintain a time-averaged repetition rate 2 Hz. Based on the MOMA laser ETU, which meets the form, fit and function of the flight laser, the stability of the output energy is approximately 10% relative standard deviation (RSD) over 2 s. The nanosecond laser pulse width allows a controlled amount of energy to be deposited on the sample, briefly heating the surface up to a few thousands of degrees, resulting in both photochemical and photothermal desorption, volatilization and ionization of atomic and molecular species. The martian atmosphere serves to rapidly lower the high initial kinetic energies of the laser-generated ions. Through incremental laser power control, the desorption threshold of complex organic molecules in geological samples can be approached slowly, limiting LDI fragmentation that develops quickly above this material-specific threshold. In addition, instrument calibration and flight-equivalent MOMA testbed operations enable the recording and interpretation of molecular interactions between desorbed ions, neutrals and ambient atmosphere, which result from the elevated temperatures and electron number densities (up to >10<sup>18</sup> cm<sup>-3</sup>) associated with transient laser-induced plasmas produced by ns-class laser systems [24].

In order to efficiently transmit the ions from Mars ambient pressure into the LIT (for which technical details are provided Section 4.1), MOMA relies on a gas conductance-limiting ion

guide with an inline fast actuating aperture valve (see Sections 4.2 and 4.3). The valve allows a burst of both analyte ions and neutral Martian atmosphere to be introduced into the analyzer chamber, resulting in a transient spike in pressure up to 10 Pa. Because mass spectral analysis requires high-voltage applied to electrodes within the LIT (down to  $-1000$  Vpp) and detector chains (down to  $-5000$ V), this pressure pulse is too large for the experiment to proceed immediately. Instead, the ions must be maintained within the LIT at a low trapping voltage until the valve is closed and the Wide Range Pump (WRP, heritage from SAM [25]) returns the chamber pressure to  $10^{-1}$  Pa. In this way, MOMA performs LDI-MS at Mars ambient pressures without needing to seal and evacuate a sample-containing volume, thereby reducing the mass, volume, power, and technical risk of the instrument. To ensure the safe activation of high-voltage electrodes and optimum “cooling” performance of the instrument, and to mitigate any reduction in instrument (filament and detector) lifetime by operating at elevated pressures, the pressure in the mass spectrometer chamber is monitored during the experiment sequence by a MEMS Pirani pressure sensor (see Section 4.4).

The duty cycle of the LDI-MS mode of operation, approximately one spectrum every 1–2 s, is primarily driven by the time it takes to pump the mechanical housing back down to vacuum after the valve is closed. To avoid over-filling the ion trap, which has a finite capacity for molecular ions, the experimental sequence is controlled by an automated algorithm wherein the laser energy and number of laser shots are increased step by step from minimal initial settings until an appropriate trap ion filling level has been reached.

The MOMA instrument also enables ion isolation and enrichment, and subsequent structural characterization of complex molecules in LDI-MS mode using multi-frequency waveforms, such as in the Stored Waveform Inverse Fourier Transform (SWIFT) [26] method, and tandem mass spectrometry (MS/MS), respectively (see Section 5.2). SWIFT allows for the isolation of a specific mass range window for enhanced signal detection, and MS/MS allows for the fragmentation of single parent molecule into a series of product ions. These techniques could help to identify diagnostic functional groups and thereby the potential origin and degree of environmental processing of compounds in the martian near surface. The overall MOMA instrument, including the key components described below, is shown in Fig. 1, and a schematic timing diagram for a typical LDI-MS experiment is provided in Fig. 2.

There are multiple mission-related factors that have the potential to impact the mass resolution, ion trapping efficiency and capacity, dynamic range and sensitivity of the MOMA mass spectrometer. These include its operation in the harsh martian environment with its low-and-variable pressure CO<sub>2</sub>-rich atmosphere and its large diurnal temperature variations, as well as under limited mass, power, volume, and data rate constraints. Moreover, the physico-chemical nature of the LDI process has intrinsic uncertainties when applied to essentially unknown (a priori) samples. The MOMA engineering test unit (ETU) and flight model (FM) have nevertheless been shown to meet all the performance requirements set by the mission. Specifically, during the LDI-MS operations, MOMA meets the following specifications:

- Identify nonvolatile molecules between 100 and 1000 Da in mass (in comparison, the mass range for GC-MS is 50–500 Da);
- Detects  $1 \text{ p} \text{mol}/\text{mm}^2$  analyte with  $\text{SNR} \geq 3$  (Rhodamine 6G and Angiotensin II have been used as standards for this requirement);
- Achieve a mass resolution such that  $m \pm 1 \text{ Da}$  up to  $m = 500 \text{ Da}$ , and, for LDI-MS,  $m/\Delta m \geq 500$  (FWHM) above this;
- Achieve dynamic range  $\geq 100$  over 50 – 1000 Da mass range in a single scan;
- Have  $\pm 5 \text{ Da}$  precision for mass isolation over 50 – 1000 Da;
- Retain mass accuracy within  $\pm 0.4 \text{ Da}$  of the actual mass;
- Have instrument mass drift  $< 0.4 \text{ Da}$  over an entire experimental cycle.

## 4. Instrument description

### 4.1. Miniaturized linear ion trap (LIT)

The measurement requirements levied on MOMA, when taken together, make an ion trap an ideal choice for the mass analyzer. Specifically, MOMA has to be compact, able to operate under only moderate vacuum conditions, be compatible with different ion sources, and be capable of MS/MS operation in order to confirm chemical identification of analytes. The capability to capture and trap ions at relatively high pressures is critical as this capability ultimately enables LDI-MS operations at Mars ambient pressures (in conjunction with the instrument's aperture valve). These requirements resulted in the selection of a linear ion trap over a more conventional quadrupole or time-of-flight mass analyzer. Unlike the 3D-type ion traps flown on the ISS and Rosetta, the LIT developed for MOMA supports symmetrical ion injection pathways through both ends of its hyperbolic rod subassembly, thereby enabling: i) two independent ion sources, namely pyr/GC-MS via electron ionization and pulsed LDI-MS; ii) redundant detection channels, thereby increasing the lifetime of the instrument and reducing technical risk; and iii) reduced space-charge effects, enhanced trapping efficiencies and a greater ion capacity compared to 3D traps with comparable physical volumes. Moreover, MOMA's LIT requires only minor modifications of the hyperbolic rod electrode assemblies flown on a number of heritage quadrupole mass spectrometer (QMS) instruments.

The MOMA LIT electrode assembly design and geometry is derived from the Thermo Fisher Scientific (hereafter Thermo) LXQ instrument [27], a discontinued version of the popular LTQ instrument from Thermo. The primary difference is that the LXQ (and by extension MOMA) uses single set of hyperbolic rod segments to define the ion trap rather than the three such segments as used in the LTQ configuration; Although the single segment design is less ideal (e.g., reduced mass resolution) due to the non-ideal fringe fields at each end of the trapping rods, this geometry enables simplified radio frequency (RF) drive electronics as well as a more compact mechanical footprint. The primary radial trapping dimension ( $r_0$ ) for the MOMA LIT was selected as 3 mm versus 4 mm for the Thermo design in order to decrease the analyzer volume (75% reduction compared to the LXQ) and reduce power requirements for a given mass range.

The available mass range for an ion trap operated in the resonance ejection mode [28] is dictated by the Mathieu equation for the dimensionless quantity  $q$ :

$$q_x = \frac{-4eV}{mr_0^2\Omega^2}$$

This equation describes the relationship between radial trapping dimension ( $r_0$ ), operating angular frequency ( $\Omega$ ), operating RF zero-to-peak voltage ( $V$ ), beta ( $\beta$ ) ejection point ( $q$ ), and ion mass-to-charge ratio ( $m/z$ );  $q$  is related to  $\beta$  in a nonlinear but continuous fashion. The key here is that all of the above parameters are interrelated and need to be considered together when designing and building a miniaturized ion trap system. When compromises are made in one place, they will have impacts in the others, and vice versa. In the case of MOMA, there are two desired operating mass ranges – pyr/GC-MS mode requires  $m/z$  50–500 with  $< 1$  Da peak widths, whereas LDI-MS mode requires  $m/z$  100–500 with  $< 1$  Da and 501–1000 with  $< 2$  Da peak widths. Tied into this is the desire to reduce the RF supply power consumption (i.e. max operating voltage) as well as the overall instrument mass and volume as much as possible. These two synergistic goals led to the reduction in  $r_0$  down to 3 mm – resulting in a higher ultimate mass range for a given maximum RF voltage as compared to the 4 mm design. Performance testing of the MOMA trap at various RF frequencies and  $\beta$  ejection points produced an optimized set of operational parameters, which are outlined in Table 1. Using these conditions, MOMA meets all of its measurement requirements, as outlined in [Section 5], while fitting within the flight constraints.

#### 4.2. Aperture valve

The MOMA aperture valve enables LDI-MS at Mars ambient pressure without requiring a vacuum seal to the sample. This interface also ensures constant pressure during pyr/GC-MS experiments (0.4 Pa or 3 mTorr, He background gas) and vacuum ( $< 10^{-4}$  Pa) during high-voltage preconditioning of the detectors and dynodes and high-temperature cleanup operations aimed at reducing the accumulation of potential contaminants. The valve design and overall LDI-MS experimental sequence is inspired by the discontinuous atmospheric pressure ionization (DAPI) pioneered by researchers at Purdue University [29]. The MOMA valve implementation has design requirements and features particular to Mars science and spaceflight reliability concerns. For example, the MOMA valve employs a check ball sealing mechanism consisting of a precision sapphire ball that fits into a tightly toleranced valve seat (Figs. 3 and 4). The valve body is machined from single piece of nonmagnetic Ni-Co based MP35N alloy. The slide that carries the spring-loaded sapphire ball, on the other hand, is composed of chemically resistant Nitronic 60 stainless steel to inhibit galling, wear and corrosion.

The valve is actuated by a pull-type solenoid that requires less than 5 W peak power ( $< 0.5$ W average) and opens and seals the inlet within 10 ms and 20 ms, respectively. A magnet embedded in the valve slide and a Hall sensor positioned at the opposite end of the solenoid provide telemetry on valve function. The size of the valve, inclusive of the solenoid, is highly compact: approximately 96 mm (length)  $\times$  24 mm (width)  $\times$  20 mm (height), and weighs  $< 100$ g. The valve has been life tested in excess of 160,000 cycles, and it carries an

end-of-life leak rate requirement of  $<10^{-5}$  cc/sec of He at atmospheric pressure, and an operational temperature range of  $-35$  to  $+25^{\circ}\text{C}$  (based on thermal predictions plus qualification margins). The valve design has been qualified for spaceflight, and specifically the MOMA investigation, through the following battery of tests: i) vibration testing to MOMA-specific loads; ii) thermal cycling between survival temperatures ( $-55^{\circ}\text{C}$  to  $+125^{\circ}\text{C}$ ); iii) lifetime testing ( $>130,000$  actuations, meeting  $2\times$  mission lifetime requirements) in a realistic environment, including during active particulate sample irradiation with a pulsed laser source that simulated the MOMA flight laser; and, iv) leak rate verification before and after all of these qualification tests.

### 4.3. Ion inlet tube and ion introduction

The aperture valve is effectively a vacuum gate valve in series with a capillary ion inlet tube (Fig. 4), which serves to limit the conductance between Mars ambient pressure and the actively-pumped MS housing when the valve is open. The inlet tube allows transport of the desorbed ions into the ion trap, via entrainment in the flow of Mars atmospheric gas through the ion inlet tube, and transferred into the LIT. Experiments were performed to optimize transfer during this dynamic sequence, specifically investigating ion transmission efficiency versus the length and inner diameter of the inlet tube (see Fig. 5). Initial selection of suitable tube dimensions was made based on the Simulink-based MOMA experiment SIMulator (MOMASIM) model of the vacuum system, anticipated pressure load, and targeted pump down time. The conductance of each gas transfer element was dynamically computed using the Knudsen empirical formula as a function of the element dimension, gas composition, pressure and temperature. The Mars pressure at the possible landing sites for the ExoMars Rover, including seasonal and diurnal variations, is expected to be in the range  $0.5\text{--}1$  kPa (or  $4\text{--}8$  Torr) [23], but physical experiments were performed over a wider range to validate the model and better understand the relationship between Mars pressure and analytical performance. Quantitative comparison between the model and the actual gas processing system of MOMA showed that this formula provides gas flow parameters accurate to within 20%. As shown in Fig. 5 and as expected based on the equation for the conductance  $C$  of a tube ( $c \propto \text{diameter}^4/\text{length}$ ), tubes with smaller inner diameters required higher Mars atmospheric pressures to transmit ions than tubes with larger inner diameters. Shorter length tubes supported effective ion transmission across a wider range of pressures compared to longer tubes, likely due to fewer collisional losses to the tube walls. Selection of the final tube dimensions was made based on: i) these data (ion transmission efficiency); ii) constraints on the tube length imposed by the mechanical dimensions of the aperture valve and the volume envelope of the MOMA accommodation within the ExoMars Rover; and, iii) the acceptable gas loading on the WRP. A tube length of 3 cm and inner diameter of 1.3 mm was determined to be an optimal compromise.

Several other important operational parameters related to the LDI process were also studied early in this development. The distance between the sample and the ion inlet tube was found to be crucial in determining the sensitivity of the ion source, with closer spacing exhibiting significantly higher sensitivities. Mechanical tolerance limitations at MOMA's interface to the ExoMars rover sample handling system limited this distance to a minimum of 3 mm. Therefore 3 mm was selected as the nominal sample-to-tube distance. Tests show that an



increase in this distance to 4 mm results in a loss of ~30% of the ion signal, dependent on the sample type, laser and voltage conditions. Likewise, decreasing this distance to 2mm can more than double the signal levels in some cases. A mass-dependent transfer mechanism was also observed when studying lower masses with this interface. The observed ion intensities gradually decreased, starting at  $m/z$  100 down to  $\sim m/z$  85 where signal intensity effectively reached instrument baseline. Higher mass ions did not show transfer issues and were efficiently transferred and trapped, provided sufficient RF voltage was used for higher mass trapping. This effect was separate from the known and expected low mass cut off effect that is present in all ion traps, i.e. lowering the RF voltage during trapping did not result in an increase in the low mass signal. It is not clear if this mass-dependence is occurring in the gap between the sample and the inlet tube or within the inlet tube itself; however, the primary goal for LDI on MOMA is to analyze higher mass organic species where the detection of lower mass (more volatile organics) species can be corroborated via pyr/GC-MS. Finally, due to the dynamic nature of this mode of operation, the transferred ions need to be maintained in the trap during the pump down of the excess Mars gas before mass analysis. Simulations showed pump down times of  $\sim 1$  s were required to reach 0.07 Pa (or 0.5 mTorr). This result was confirmed experimentally via pump down curve measurements from the ETU and FLT instruments (see Fig. 4C). Extended experiments showed that ions could survive for several seconds without experiencing significant degrees of neutralization, fragmentation or ion-molecule reactions. Consequently, the selection of an ion trap mass analyzer has been validated through the implementation of this dynamic experimental sequence.

#### 4.4. MEMS pirani sensor and dynamic pumpdown curve

MOMA relies on a Microelectromechanical System (MEMS) Pirani sensor for pressure monitoring. The two operational modes of the MOMA instrument require the sensor to measure both the static pressure of Helium in the 0.4Pa (or 3mTorr) range (pyr/GC-MS mode) as well as the dynamic pressure pulses induced during LDL-MS mode. During LDL-MS operations, the pressure in the MOMA-MS may transiently increase to 7 Pa (or 50 mTorr) during which time no voltage higher than 250 VDC ( $100 V_{RF0-p}$ ) is applied inside the MS, due to the risk of coronal discharge. To minimize signal loss associated with limited ion lifetime, the high-voltage detectors and dynodes are activated and the analytical RF ramp initiated as soon as possible after the pressure drops below the 0.07 Pa (or 0.5 mTorr) safety threshold. As a result, the MOMA-MS pressure sensor needs to accurately measure pressures in the 0.01–7 Pa (or 0.1–50 mTorr) range of the Mars mix and exhibit fast response times (0.25 s), all while meeting the mission lifetime, shock, vibrate, and operational temperature ( $-50$  to  $80$  °C) requirements. Pressure measurement capabilities of the MOMA-MS sensor are detailed in Table 2.

In contrast to MOMA, previous generations of planetary mass spectrometers (e.g., the SAM QMS on MSL [14]) employed Bayard-Alpert (hot filament) ion gauges to measure pressure; these types of transducers, however, are not suitable for pressures over 0.1 Pa (or 1 mTorr), and therefore alternatives were explored during the initial design of MOMA. While MEMS pressure sensors have flown on the Rosetta mission [30], MOMA is the first instrument to employ a MEMS Pirani pressure gauge, enabled by recent improvements in the

ruggedization and sensitivity of such sensors, which extended their operational range down to pressures in the mTorr-pTorr regime [31]. As their name indicates, these gauges are very small (9.2 mm diameter), light-weight (1 g) and use less than 300  $\mu$ W, making them ideal candidates for portable, hand-held mass spectrometers and/or instrumentation for planetary exploration (See insets in Fig. 6.)

To meet the MOMA pressure monitoring requirements (Table 2) the Heimann HVS-03 K MEMS Pirani sensor was chosen over the HVS-03G model due to its faster response. This sensor contains a sense resistor ( $R_p$ ) embedded in a silicon nitride membrane whose temperature depends on pressure and ambient temperature. A separate, compensator resistor ( $R_k$ ) is used to actively monitor and properly compensate for ambient temperature variations (See inset in Fig. 6 for  $R_p$  and  $R_k$ ).

Accelerated lifetime experiments were performed to determine a suitable bias voltage across the combined resistance of the sense and compensator resistors; in general, higher bias voltages produce more wear (sensitivity degradation) on the device but also improved signal to noise ratio. Thirty Pirani sensors were biased at voltages of 1.6, 2.1, and 2.6V and the drift of the sense resistor resistance ( $R_p$ ) was monitored over time as the indicator of the Pirani wear. High ambient temperatures and operating voltages were found to induce most wear on the Pirani sensors. A subsequent life test with nine flight Pirani sensors biased at 2.1 V in the ambient temperature of 100 $^{\circ}$ C (significantly higher than the maximum operational temperature of 80  $^{\circ}$ C) over 930 h ( $\sim 1 \times$  mission life) showed less than 0.31% drift, thus translating into a pressure error smaller than 0.01 Pa (or 0.1 mTorr) and meeting the strenuous static pressure accuracy requirement for the entire mission lifetime.

The dynamic pressure response of the MOMA-MS MEMS Pirani sensor was tested with flight electronics (including a 250mW Pirani sensor control circuit) under realistic pressure conditions MOMA-MS experiences during LDMS operations. For this purpose, a pulsed solenoid valve was used to briefly introduce a short  $\sim 100$ – $200$  ms pressure pulse of the Mars mix into a vacuum test chamber pumped by a turbo pump throttled to match flight-like WRP pumping conditions. The chamber was outfitted with a thermo-electric cooler (TEC) for control of the ambient temperature over the expected operational temperature range of the sensor ( $-50$  to  $80$   $^{\circ}$ C). Comparison of the typical dynamic pressure response of the MEMS Pirani with that of the calibrated capacitance manometer (MKS Instruments, Baratron $^{\circ}$ , Model 626–0.1 Torr) is shown in Fig. 6.

## 5. Results and discussions

### 5.1. Performance metrics for the MOMA ion trap

As described above, the design of the MOMA linear ion trap mass spectrometer and supporting electronics is a balance between the required performance to meet top-level science requirements for the detection of organic species in Martian regolith and the stringent mass, power, and volume limitations inherent to spaceflight instruments. In order to characterize the ion trap performance, two calibration compounds are used as part of ground-based test campaigns. Single crystal, solid CSI is pressed into a titanium sample holder placed in a chamber with a controlled environment meant to simulate Mars

atmospheric conditions (pressure and gas composition). In this “Mars chamber”, the sample is interrogated by a variable number (1–20 shots in a “burst”) and energies (13–130 uJ) of the 266nm Nd:YAG laser. Here, mass spectra arising from the analyses of CSI (Fig. 7(A)) demonstrate the performance requirements for mass range, mass resolution and mass accuracy. A CSI calibration target coated in a thin film of gold to reduce hygroscopicity will be carried in the *flight* carousel to allow for the mass calibration and assessment of performance of LDI mode while on the surface of Mars.

In order to demonstrate the performance (specifically sensitivity) of the MOMA linear ion trap to detect organic molecules, an organic dye, Rhodamine 6G, was dropcast onto a titanium sample stub at a concentration of 50 fmol/mm<sup>2</sup>. While the requirement for sensitivity to organic molecules is 1 pmol/mm<sup>2</sup>, care must be taken not to introduce unnecessary amounts of any organic molecules to the mass spectrometer to eliminate chances of carry-over or contamination of surfaces in the vacuum chamber. Fig. 7(B) shows the mass spectrum that arises from the interrogation of 50 fmol/mm<sup>2</sup> of R6G.

Note that the above examples are meant as characterization studies to prove the functionality and performance of the LDL mode of operation of MOMA. These controlled sample conditions are not fully representative of the complex matrices that may be experienced on Mars. Multicomponent organic/mineral mixtures are currently being investigated in order to better understand chemical signals derived from progressively more complex analog samples and to validate the experimental protocols that will be used to deal with such samples. In addition, we also demonstrated previously [11] that LDI-MS mode provides distinct advantages for detecting organics *in situ* on the Martian surface. Specifically, the detection of trace amount nonvolatile organics in minerals is not inhibited by the presence of up to 1 wt.% perchlorate salt, which is believed to exist on Mars surface globally [32]. In contrast to the results from pyr/GC-MS of organic molecules in the presence of perchlorate, LDL produces mass spectra that retain the intact parent molecular ion without the presence of thermally driven reactions and subsequent decomposition.

## 5.2. Advanced analytical capabilities of the MOMA ion trap

The complexity of the ion signature arising from laser desorption of Mars-like analogs requires specialized techniques to ensure optimal spectral performance from the miniaturized analyzer. To help manage this complexity, ions of a particular mass range of interest can be selectively trapped, to both eliminate the contribution from matrix ions and to enhance potential analyte signal. The MOMA ion trap is equipped with digital auxiliary waveform injection capabilities in support of the SWIFT technique. While several waveforms will be stored on the flight instrument memory, allowing for predetermined, automated SWIFT analyses as a baseline, additional customized waveforms can be implemented, ground-tested, and sent to the rover once it is on Mars.

The SWIFT technique can be employed in several scenarios during LDI-MS operations on Mars. During the start of every LDI-MS cycle, the experiment control script will gradually increase the laser power and number of shots to attempt to achieve optimum ion loading (i.e. optimum peak S/N but no trap overloading causing a reduction in mass spectral performance). This amounts to an automatic gain control (AGC) algorithm designed to

operate within the reproducibility and uncertainty confines of the LDI process. Once proper ion trap loading has been achieved situations may still exist where particular mass ranges are dominating the trapped ion density. In these cases, SWIFT “windows”, with widths of 100, 200 or 300 Da, can be used to selectively trap only ions within the chosen band. Alternately, if a potentially interesting ion is observed in the initial optimized spectrum (e.g. high intensity or high mass peak), a smaller SWIFT\* window can be employed for specific ion enrichment. We have found that with proper waveform frequency and amplitude tuning it is possible to implement SWIFT\* isolation during ion injection when the trap pressure is  $\gg 0.4$  Pa (or 3mTorr). While SWIFT resolution is significantly degraded due to pressure broadening, it is more than adequate for coarse filtering during ion loading allowing enhancement of a mass range of interest. Fig. 8 provides an example of SWIFT ion enrichment. The first spectrum (Fig. 8(A)) represents an LDI-MS spectrum of an example polyaromatic hydrocarbon (10 ppm coronene,  $[M]^+ = 300$  Da) doped into an iron-rich Martian clay analog, nontronite. Here the spectrum shows significant low mass contribution from the mineral matrix, while the analyte parent ion peak at 300 Da is present in low abundance. After applying the SWIFT waveform to eliminate all masses below  $\sim m/z$  225 (Fig. 8(B)), the total ion counts are dramatically reduced while still selectively trapping the coronene protonated molecular species. Successive increase in the laser AGC settings (in the case of Fig. 8(C) increasing the number of laser shots) allows for the optimal trap loading while enhancing ion signal from the trapped SWIFT window.

A second application of the SWIFT technique is demonstrated with the analyses of simulated Mars regolith samples. The intensity and complexity of the signal that arises from terrestrial analogs of Martian crushed rock samples illustrates the need for methodology to control the ion loading in the mass spectrometer. Indeed, the mass spectrum displayed in F 9 (black) shows the mass spectrum acquired on a silicate mineral, Enstatite. Here, the acceptable ion trap capacity is exceeded, producing broadened and shifted mass spectral peaks due to space charge effects. The top plot (blue) shows how resolution and mass accuracy can be maintained by using SWIFT to control the ion loading of the MS. By only trapping a selected window of ions, the ion trap capacity can be more efficiently utilized to produce higher SIN for the selected mass range without overloading. While one section of the mass spectrum alone may not fully describe a collected sample, taking spectra across several mass range windows (e.g.,  $m/z$  150–250 as shown In Fig. 1) and stitching together the spectra can elucidate the full mass range without degradation of MS performance. Because each laser pulse removes only  $<10$  nm of material [33], the sample (or more specifically, the assemblage of phases situated underneath the laser beam) may be considered relatively homogeneous across several collected mass spectra.

SWIFT is also used on the MOMA ion trap for isolation of species prior to MS/MS analysis. In LDI mode, this provides another critical piece of information for the elucidation of an ions structure, similar to what chromatographic separation provides for in EI mode. Due to the dynamic Mars gas pressure present during MOMA’s LDIMS mode of operation, MS/MS analysis must be performed at key times within the pump down profile. Coarse isolation can be implemented during ion trapping to enhance the parent ion intensity, but fine isolation (specified as a 10 Da isolation width) with SWIFT was found to only be possible after the APV has closed and the instrument has pumped down to  $<2.7$  Pa (or 20 mTorr). Parent ions

are then excited via a ramped amplitude, single frequency excitation causing energetic collisions with the background Mars gas (primarily CO<sub>2</sub>) at MS housing pressures of 1.3–0.13 Pa (or 10–1 mTorr). The ramped amplitude has been found to provide sufficient flexibility in the excitation energy application that the dynamic pressure during this stage does not detrimentally affect MS/MS performance or efficiency. After fragmentation, product ions are re-trapped and cooled by the remaining Mars gas. Finally, after the pressure has dropped below 0.07 Pa (or 0.5 mTorr), the products are ejected and detected, as in standard LDI-MS mode, but now producing an MS/MS spectrum. Fragmentation of the [M + H]<sup>+</sup> parent ion (*m/z* 1046.5) of the peptide Angiotensin II, dropcast onto a titanium sample stub in the presence of 2,6-dihydroxybenzoic acid (DHB), is shown in Fig. 10, demonstrating the MS/MS capabilities of MOMA. The mass spectrum shows efficient fragmentation of the parent, with characteristic b- (N terminal fragment) and y-type (C terminal fragment) ions commonly observed in peptide MS/MS analysis. Though not part of MOMA's baseline capabilities, the instrument is capable of further stages of tandem mass spectrometry (i.e. MS<sup>n</sup>) to provide additional structural information for ions of interest.

## 6. Conclusion and outlook

The mass spectrometer, MOMA, is a key instrument on the ExoMars Rover mission and has been designed, built, and optimized specifically for operation within the harsh Martian environment. The miniaturized LIT mass spectrometer coupled to a Mars-optimized LDI source represents an innovative and novel technique for characterizing surface material and searching for signs of life—potential high molecular weight organics biosignatures, even in the presence of oxychlorine compounds. The LDI-MS mode of operation, combined with SWIFT and MS/MS techniques, enable structural information to be derived from the Martian samples *in situ*. The instrument provides a great opportunity to probe the full organic inventory at Mars which beyond the immediate science of ExoMars will in turn advise analytical capability requirements for Mars Sample Return (MSR).

The development of MOMA for the ExoMars mission has allowed for the maturation of several technologies and techniques surrounding the LDI-MS mode of operation that are new to robotic space exploration. This work has also highlighted further enhancements that are possible and are currently being implemented in the next generation “MOMA-like” instrument for use exploring other planets and solar system targets as well as unique earth applications. The Linear Ion Trap Mass Spectrometer (LITMS), is based on the MOMA instrument design but adds the ability to directly analyze rock core samples along with dual polarity ion detection and expanded low and high mass range operation. In addition to full test campaigns for LITMS in a laboratory and simulated Martian environment, it will also be tested on a demonstration rover in the Atacama Desert. The unique capabilities of the LIT and its LDI-MS mode of operation will continue to be developed and optimized and will substantially benefit the exploration of a variety of environments by providing significant and meaningful scientific return.

## References

- [1]. Robotic Exploration of Mars, European Space Agency. <http://exploration.esa.int/mars/> (accessed on May 22nd. 2017).
- [2]. Brinckerhoff WB, Pinnick VT, van Amerom FHW, Danell RM, Arevalo RD, Atanassova MS, Xiang L, Mahaffy PR, Cotter RJ, Goesmann F, Steininger H. Mars organic molecule analyzer (MOMA) mass spectrometer for ExoMars 2018 and beyond, Aerospace Conference, 2013 IEEE (2013) 1–8.
- [3]. Pavlov AA, Vasilyev G, Ostwakov VM, Pavlov AK, Mahaffy P, Degradation of the organic molecules in the shallow subsurface of Mars due to irradiation by cosmic rays, *Geophys. Res. Lett* 39 (2012) n/a-n/a.
- [4]. Chutjian A, Bornstein BJ, Conroy DG, Croonquist AP, Darrach MR, Overview of the Vehicle Cabin Atmosphere Monitor, a Miniature Gas Chromatography/Mass Spectrometer for Trace Contamination Monitoring on the ISS and CEV, Society of Automotive Engineers, Warrendale Penn 2007.
- [5]. Andrews D, Barber S, Morse A, Sheridan S, Wright I, Morgan G. Ptolemy An instrument aboard the Rosetta lander Philae, to unlock the secrets of the solar system, in: 37th Lunar and Planetary Science Conference, Houston, Texas USA, 2006.
- [6]. Vastola FJ, Mumma RO, Pirone AJ, Analysis of organic salts by laser ionization, *Org. Mass Spectrom* 3 (1970) 101–104.
- [7]. Tanaka K, Ido Y, Akita S, Yoshida Y, Yoshida T, Detection of high mass molecules by laser desorption time-of-flight mass spectrometry, Second Japan-China Joint Symposium on Mass Spectrometry (1987) 185–188.
- [8]. Karas M, Hillenkamp F, Laser desorption ionization of proteins with molecular masses exceeding 10.000 daltons. *Anal. Chem* 60 (1988) 2299–2301. [PubMed: 3239801]
- [9]. Apicella B, Carpentieri A, Alfè M, Barbella R, Tregrossi A, Pucci P, Ciajolo A, Mass spectrometric analysis of large PAH in a fuel-rich ethylene flame, *Proc. Combust. Inst* 31 (2007) 547–553.
- [10]. Rizzi A, Cosmina P, Flego C, Montanari L, Smaniotto A, Seraglia R, Traldi P, Laser desorption/ionization techniques in the characterization of high-molecular-weight oil fractions–Part 2: de-asphalted oils, *J. Mass Spectrom* 42 (2007) 874–880. [PubMed: 17534858]
- [11]. Li X, Danell RM, Brinckerhoff WB, Pinnick VT, van Amerom F, Arevalo RD, Getty SA, Mahaffy PR, Steininger H, Goesmann F, Detection of trace organics in mars analog samples containing perchlorate by laser desorption/ionization mass spectrometry, *Astrobiology* 15 (2015) 104–110. [PubMed: 25622133]
- [12]. Niemann HB, Hartle RE, Kasprzak WT, Spencer NW, Hunten DM, Carignan GR, Venus upper atmosphere neutral composition: preliminary results from the pioneer venus orbiter, *Science* 203 (1979) 770–772. [PubMed: 17832991]
- [13]. Mahaffy PR, Richard Hodges R, Benna M, King T, Arvey R, Barciniak M, Bendt M, Carigan D, Errigo T, Harpold DN, Holmes V, Johnson CS, Kellogg J, Kimvilakani P, Lefavor M, Hengemihle J, Jaeger F, Lyness E, Maurer J, Nguyen D, Nolan TJ, Noreiga F, Noriega M, Patel K, Prats B, Quinones O, Raaen E, Tan F, Weidner E, Woronowicz M, Gundersen C, Battel S, Block BP, Arnett K, Miller R, Cooper C, Edmonson C, The neutral mass spectrometer on the lunar atmosphere and dust environment explorer mission, *Space Sci. Rev* 185 (2014) 27–61.
- [14]. Mahaffy PR, Webster CR, Cabane M, Conrad PG, Coll P, Atreya SK, Arvey R, Barciniak M, Benna M, Bleacher L, Brinckerhoff WB, Eigenbrode JL, Carignan D, Cascia M, Chalmers RA, Dworkin JP, Errigo T, Everson P, Franz H, Farley R, Feng S, Frazier G, Freissinet C, Glavin DP, Harpold DN, Hawk D, Holmes V, Johnson CS, Jones A, Jordan P, Kellogg J, Lewis J, Lyness E, Malespin CA, Martin DK, Maurer J, McAdam AC, McLennan D, Nolan TJ, Noriega M, Pavlov AA, Prats B, Raaen E, Sheinman O, Sheppard D, Smith J, Stern JC, Tan F, Trainer M, Ming DW, Morris RV, Jones J, Gundersen C, Steele A, Wray J, Botta O, Leshin LA, Owen T, Battel S, Jakosky BM, Manning H, Squyres S, Navarro-González R, McKay CP, Raulin F, Sternberg R, Buch A, Sorensen P, Kline-Schoder R, Cascia D, Szopa C, Teinturier S, Baffes C, Feldman J, Flesch G, Forouhar S, Garcia R, Keymeulen D, Woodward S, Block BP, Arnett K, Miller R,

Edmonson C, Gorevan S, Mumm E, The sample analysis at mars investigation and instrument suite, *Space Sci. Rev* 170 (2012) 401–478.

- [15]. Mahaffy PR, Benna M, King T, Harpold DN, Arvey R, Barciniak M, Bendt M, Carrigan D, Errigo T, Holmes V, Johnson CS, Kellogg J, Kimvilakani P, Lefavor M, Hengemihle J, Jaeger F, Lyness E, Maurer J, Melak A, Noreiga F, Noriega M, Patel K, Prats B, Raaen E, Tan F, Weidner E, Gundersen C, Battel S, Block BP, Arnett K, Miller R, Cooper C, Edmonson C, Nolan JT The neutral gas and ion mass spectrometer on the mars atmosphere and volatile evolution mission, *Space Sci. Rev* 195 (2015) 49–73.
- [16]. Niemann HB, Atreya SK, Carignan GR, Donahue TM, Haberman JA, Harpold DN, Hartle RE, Hunten DM, Kasprzak WT, Mahaffy PR, Owen TC, Spencer NW, Way SH, The galileo probe mass spectrometer: composition of jupiter's atmosphere, *Science* 272 (1996) 846–849. [PubMed: 8629016]
- [17]. Niemann HB, Harpold DN, Atreya SK, Carignan GR, Hunten DM, Owen TC, Galileo probe mass spectrometer experiment, *Space Sci. Rev* 60 (1992) 111–142.
- [18]. Niemann HB, Atreya SK, Bauer SJ, Biemann K, Block B, Carignan GR, Donahue TM, Frost RL, Gautier D, Haberman JA, Harpold D, Hunten DM, Israel G, Lunine JI, Mauersberger K, Owen TC, Raulin F, Richards JE, Way SH The gas chromatograph mass spectrometer for the Huygens probe, *Space Sci. Rev* 104 (2002) 553–591.
- [19]. Mahaffy PR, Webster CR, Atreya SK, Franz H, Wong M, Conrad PG, Harpold D, Jones JJ, Leshin LA, Manning H, Owen T, Pepin RO, Squyres S, Trainer M, M.S. Team, Abundance and isotopic composition of gases in the martian atmosphere from the curiosity rover, *Science* 341 (2013) 263–266. [PubMed: 23869014]
- [20]. Danell RM, Danell AS, L Glish G, Vachet RW, The use of static pressures of heavy gases within a quadrupole ion trap, *J. Am. Soc. Mass Spectrom* 14 (2003) 1099–1109. [PubMed: 14530090]
- [21]. Karas M, Bachmann D, Hillenkamp F, Influence of the wavelength in high-irradiance ultraviolet laser desorption mass spectrometry of organic molecules. *Anal. Chem* 57 (1985) 2935–2939.
- [22]. Vertes A, *Soft Laser Desorption Ionization-Maldi, Dios and Nanostructures, Laser Ablation and Its Applications*, Springer, US, 2007, pp. 505–528.
- [23]. Harri AM, Genzer M, Kemppinen O, Kahanpää H, Gomez-Elvira J, Rodriguez-Manfredi JA, Haberle R, Polkko J, Schmidt W, Savijärvi H, Kauhanen J, Atlaskin E, Richardson M, Siili T, Paton M, de la Torre Juarez M, Newman C, Rafkin S, Lemmon MT, Mischna M, Merikallio S, Haukka H, Martin-Torres J, Zorzano MP, Peinado V, Urqui R, Lapinette A, Scodary A, Mäkinen T, Vazquez L, Rennö N, REMS/MSL Science Team, Pressure observations of the curiosity rover: initial results, *J. Geophys. Res.: Planets* 119 (2014) 82–92.
- [24]. Liu HC, L Mao X, Yoo JH, Russo RE, Early phase laser induced plasma diagnostics and mass removal during single-pulse laser ablation of silicon, *Spectrochim. Acta Part B* 54 (1999) 1607–1624.
- [25]. Sorensen P, Kline-Schoder R, Farley R, Wide range vacuum pumps for the SAM instrument on the MSL curiosity rover. *The 42nd Aerospace Mechanism Symposium* (2014) 463–470.
- [26]. Marshall AG, Wang TCL, Ricca TL Tailored excitation for fourier transform ion cyclotron mass spectrometry. *J. Am. Chem. Soc* 107 (1985) 7893–7897.
- [27]. Senko MW, Schwartz JC, Two-dimensional quadrupole ion trap, Google Patents, (2007).
- [28]. Goeringer DE, Whitten WB, Ramsey JM, McLuckey SA, Glish GL Theory of high-resolution mass spectrometry achieved via resonance ejection in the quadrupole ion trap, *Anal. Chem* 64 (1992) 1434–1439.
- [29]. Gao L, Cooks RG, Ouyang Z. Breaking the pumping speed barrier in mass spectrometry: discontinuous atmospheric pressure interface, *Anal. Chem* 80 (2008) 4026–4032. [PubMed: 18461971]
- [30]. Graf S, Sekler J, Altwegg K, Duvet L, Rohner U, COPS – a novel pressure gauge using MEMS devices for space, in: *The 9th International Symposium on Materials in a Space Environment*, Noordwijk, The Netherlands, 2003, pp. 439–443.
- [31]. Völklein F, Grau M, Meier A, Hemer G, Breuer L, Woias P, Optimized MEMS Pirani sensor with increased pressure measurement sensitivity in the fine and high vacuum regime, *J. Vac. Sci. Technol. A* 31 (2013) 061604.

- [32]. Glavin DP, Freissinet C, Miller KE, L Eigenbrode J, Brunner AE, Buch A, Sutter B, Archer PD, Atreya SK, Brinckerhoff WB, Cabane M, Coli P, Conrad PC, Coscia D, Dworkin JP, Franz HB, Grotzinger JP, Leshin LA, Martin MG McKay C Ming DW, Navarro-González R, Pavlov A, Steele A, Summons RE, Szopa C, Teinturier S, Mahaffy PR, Evidence for perchlorates and the origin of chlorinated hydrocarbons detected by SAM at the Rocknest aeolian deposit in Gale Crater, *J. Geophys. Res.: Planets* 118 (2013) 1955–1973
- [33]. Goetz W, Brinckerhoff WB, Arevalo R Freissinet C, Getty S, Glavin DP, Siljeström S, Buch A, Stalport F, Grubisic A, Lit X Pinnick V, Danell R, van Amerom FHW, Goesmann F, Steininger H, Grand N, Raulin F, Szopa C, Meierhenrich U, Brucato JR, MOMA: the challenge to search for organics and biosignatures on Mars, *Int. J. Astrobiol* 15 (2016) 239–250.



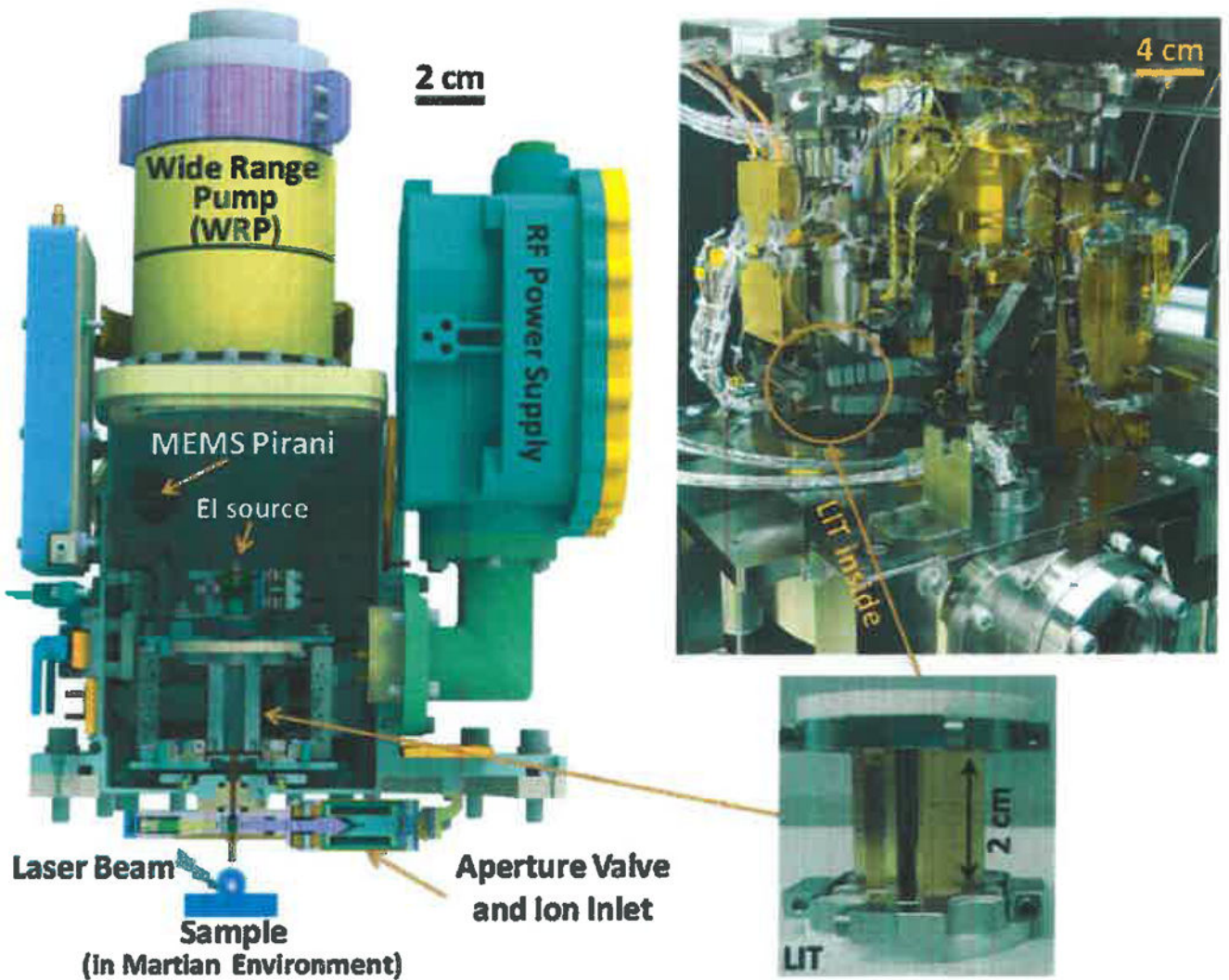


**Fig. 1.** The design of MOMA instrument. The CAD model (left) and the flight model instrument (top right). A picture of the linear ion trap (LIT) is also shown here (down right).

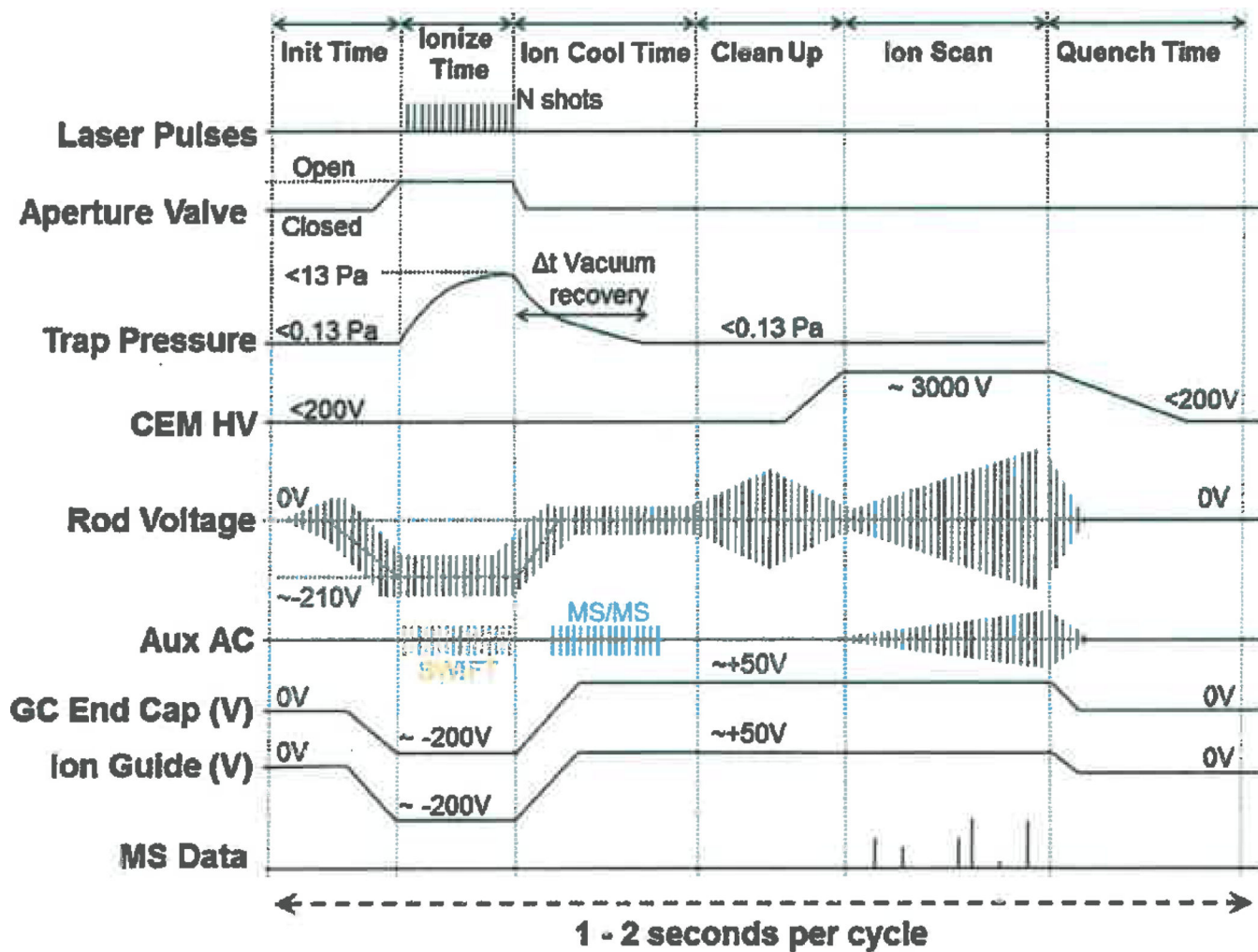
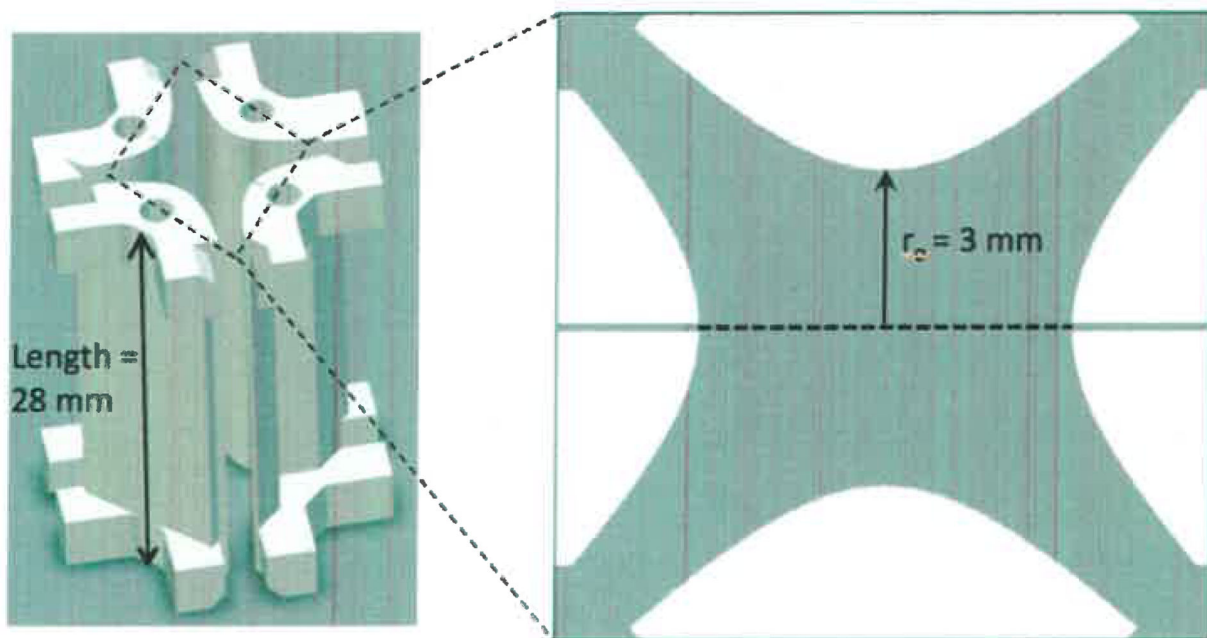
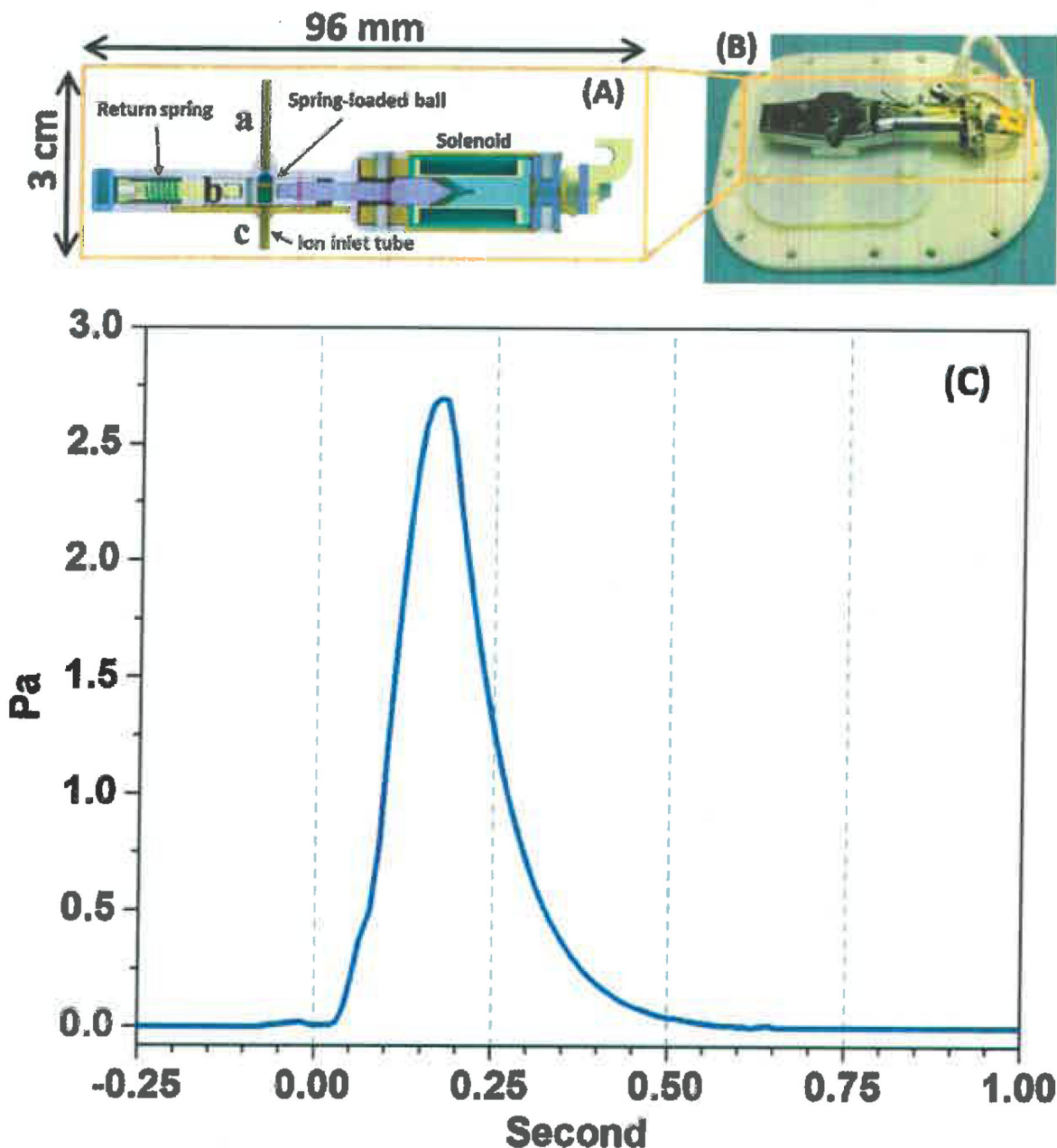


Fig. 2. The operation of the MOMA instrument in LDI-MS mode. The time (x-axis) is not to scale.



**Fig. 3.**  
The overall electrode configuration and key dimensions of the linear ion trap on MOMA.



**Fig. 4.** (A) 3D model of the cross-section of MOMA aperture valve. In this depiction, “a” indicates the vacuum side ion inlet tube with a length of 1.5 cm; “b” points to the continuation of the ion inlet tube embedded within the slide, with a tube length of 0.5 cm; and “c” shows the air-side (or Mars-side) ion inlet tube facing the sample, with a tube length of 1 cm. (B) Engineering Test Unit (ETU), or pre-flight version, of the aperture valve mounted on mockup of the interface to the mass spectrometer’s mechanical housing. (C) A recorded pressure pulse on the flight system is shown for a valve opening time of 100 ms, with Mars pressure held at 0.8 kPa (or 6 Torr) and the mass spectrometer chamber actively pumped.

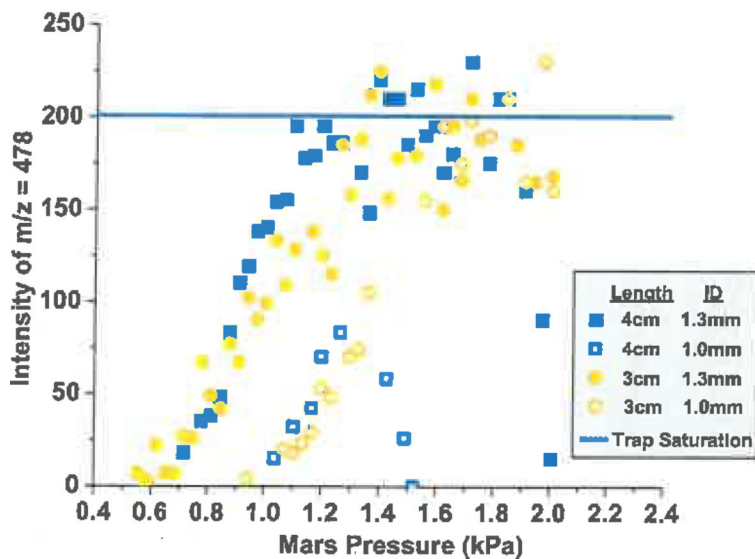
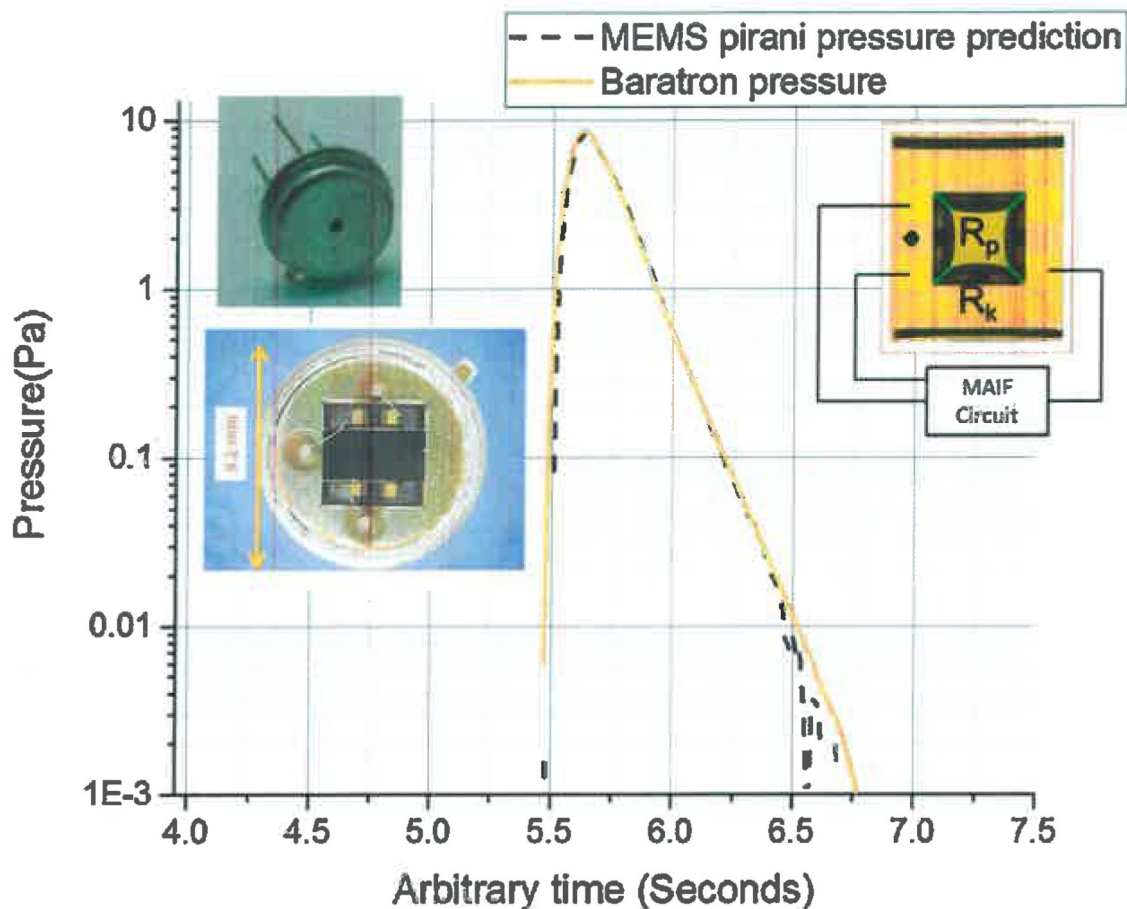


Fig. 5.

The ion counts at  $m/z$  478, the strongest ion peak in the spectra of green ink, versus the ambient pressure in sample area. Each point shown is generally an average of at least 10 spectra in order to smooth out some of the inherent shot-to-shot variability present in LDI. Tube lengths of 4cm and 3 cm, with diameters of 1.3 mm and 1.0 mm were tested (Blue squares represent the 4cm length and red circles represent 3 cm length results. The filled shapes represent 1.3 mm diameter and open shapes represent 1.0 mm diameter results). The saturation level was estimated based on ion loading performance – above this level the ion trapping efficiency starts to degrade.





**Fig. 6.**

Dynamic response of the MOMA-MS MEMS Pirani sensor (red solid line) upon actuation of the pulsed solenoid valve is compared with the capacitive pressure sensor (Baratron) measurement (black dashed line) under flight-like pumping and electronic noise conditions. Inset: (Top left) Photos of the MEMS Pirani sensor with and without the lid of the T039 package. (Top right) Photo of the sensor without the silicon microbridge [31] with  $R_p$ ,  $R_k$ , and connections to the MEMS Pirani control circuit in the flight electronics schematically indicated.

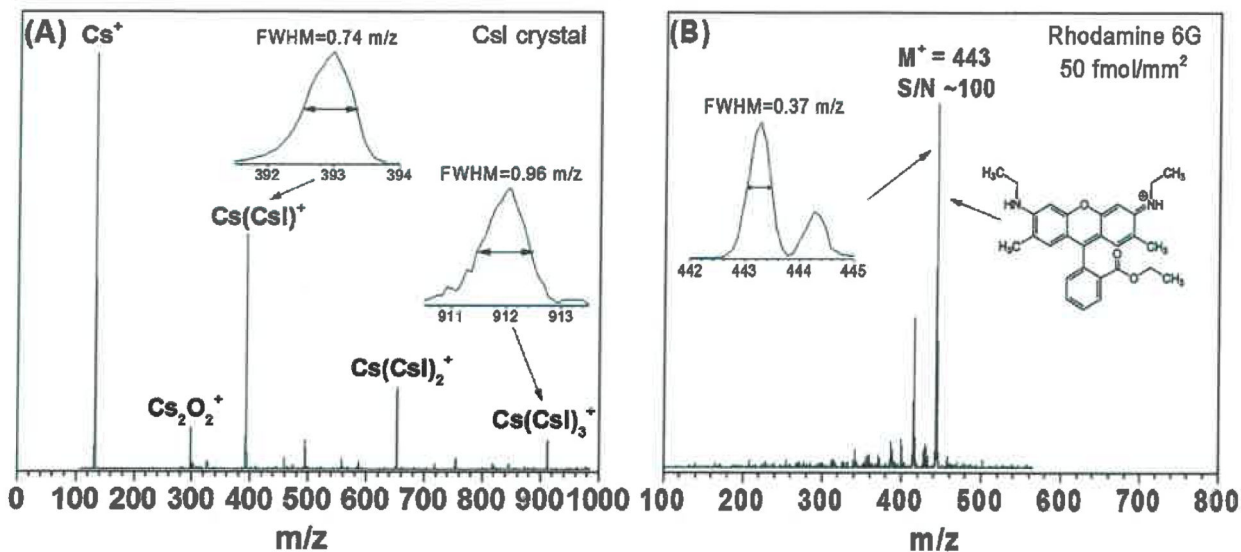


**Fig. 7.**

(a) LDI-MS spectrum acquired on the MOMA flight mass spectrometer for single-crystal CSI to demonstrate performance requirements for mass range, resolution and accuracy. (b) LDI-MS spectrum acquired on the MOMA ETU for 50 fmol/mm<sup>2</sup> R6G demonstrates high sensitivity for conjugated organics.

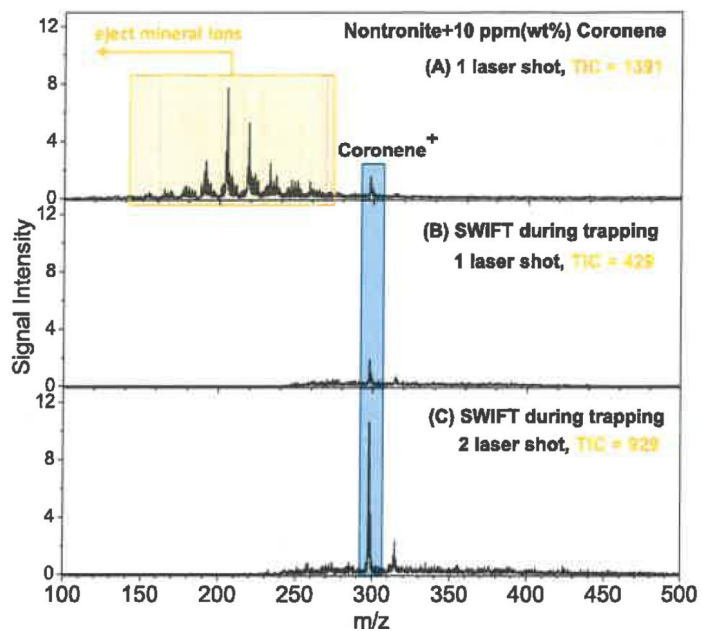


**Fig. 8.** (A) LDI-MS spectra acquired on the MOMA brassboard ion trap instrument of coronene doped nontronite. (B) isolation of  $m/z$  225–700 Da and (C) enhancement of the analyte signal with increased laser shots.



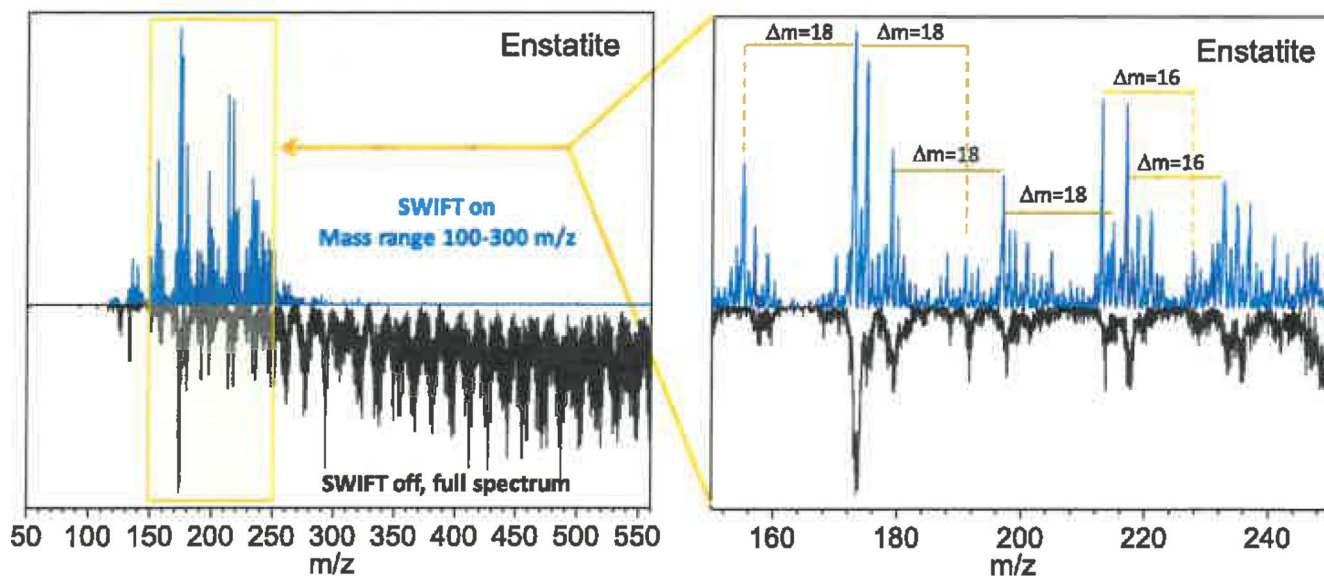


**Fig. 9.**

(A) Full mass range LDI-MS spectra acquired on the MOMA ETU instrument of Mars regolith terrestrial analog Enstatite without the use of SWIFT isolation. (B) Zoom of the central portion of the  $m/z$  100–300 SWIFT isolated mass range window demonstrating the possible improvement in the instrument performance. In both spectra the bottom, black spectra are the full mass range with no SWIFT waveform applied and the top, blue spectrum is the isolated  $m/z$  100–300 SWIFT window.

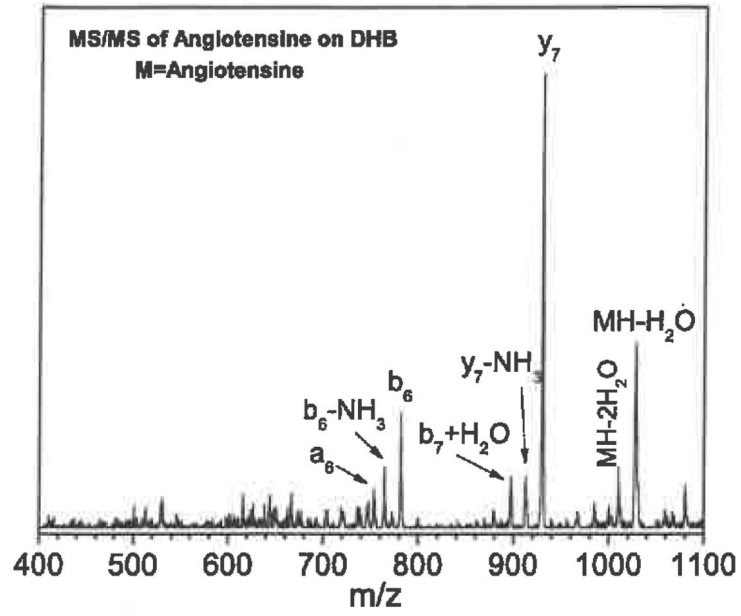


**Fig. 10.** MS/MS spectrum of Angiotensin II in DHB matrix, after isolation of the parent ion ( $m/z$  1046.5) and fragmentation via collision induced dissociation.

**Table 1**

Optimized set of operational parameters of MOMA MS.

Feature	MOMA(LIT)
$r_o$ /mm	3
Length/mm	28
RF Frequency, Voltage	1 MHz, 1200 V <sub>pp</sub> (max)
Mass Range, $\beta_{\text{eject}}$	50–500, $\beta = 2/3$ 100–1000, $\beta = 1/3$
Mass Resolution (FWHM)	<i>For m/z</i> 500, <1 Da <i>For m/z</i> > 500, <2 Da
Dynamic range	GC: 10 <sup>6</sup> (over the full chromatographic run) LDI: 100 (in a single spectrum acquisition)

**Table 2**

Performance requirements for the MOMA pressure sensor in LDI-MS mode of operation (dynamic pressure environment). The required sensor accuracy over various ranges was chosen to meet experiment and instrument operating requirements (specifically at the relatively fast response time) under the full range of mission operating conditions. They are not reflective of the ultimate performance of the sensor if fully characterized and calibrated. The required sensor response time is 0.25 s, which was chosen to match with the typical pump down time, from 50 mtorr to 0.1 mtorr, of 0.6–0.9 s.

<b>Pressure Range</b>	<b>Required accuracy</b>
5–50 mTorr	+10 mTorr/–20%
1–5 mTorr	+/-20%
0.1–1 mTorr	+/-0.2 mTorr